Novel In Situ Fabrication of Chestnut-Like Carbon Nanotube Spheres from Polypropylene and Nickel Formate

Xuecheng Chen,[†] Junhui He,*[,†] Chunxiao Yan,[‡] and Huamin Tang[‡]

Functional Nanomaterials Laboratory, Technical Institute of Physics and Chemistry, Chinese Academy of Sciences (CAS), Zhongguancun Beiyitiao 2, Haidianqu, Beijing 100080, China, and Institute of Chemical Defense, P.O. Box 1048, Beijing 102205, China

Received: July 24, 2006; In Final Form: August 29, 2006

A novel in situ approach to mass fabrication of carbon nanotubes was reported. Composites of polypropylene (PP)/organomontmorillonite (OMMT)/nickel formate (NF) were prepared by mixing these components in a Brabender mixer at an elevated temperature. Chestnut-like carbon nanotube (CNT) spheres were in situ fabricated in high yields by heating the PP/OMMT/NF composites at 900 °C without adding any additional pre-synthesized nickel nanocatalysts. The products were studied by X-ray diffractometer (XRD), transmission electron microscopy (TEM), scanning electron microscopy (SEM), Raman spectroscopy, and N_2 adsorption−desorption measurements. The results showed that nickel nanoparticles were in situ produced, which catalyzed the formation of multiwalled carbon nanotubes (MWNTs) in an autoclave-like microreactor formed by OMMT. These in situ formed nickel nanoparticles were found to be more catalytically active than pre-synthesized nickel nanocatalysts, resulting in higher yields of CNTs. The obtained CNT spheres have a high surface area, which makes them a good catalyst support. Loading of metal nanoparticles was preliminarily tried, and Pt nanoparticles of ca. 2.65 nm in size were successfully deposited on CNTs. The applications of these nanocatalysts in chemical reactions are currently being studied in our laboratory.

Introduction

Carbon nanotubes (CNTs) exhibit a series of unique properties that make them promising for many applications, such as in structural materials and electronic and optical devices.[1] Continuous, low-cost production, and easy purification of CNTs have long been much desired. A variety of synthetic methods including arc-discharge,[2] laser vaporization,[3] and chemical vapor deposition (CVD)[4] have been explored. Among them, CVD is currently the most widely used because it requires relatively low-cost equipment and is capable of producing relatively large amount of CNTs in a short time. Catalysts used for synthesizing CNTs include metallic (Ni, Co, Fe) nanoparticles loaded on a support that has commonly been used in recent years[5] and organometallic compounds such as ferrocene[6] and nickel formate.[7] Commonly used carbon sources for synthesizing CNTs are gaseous organic molecules such as CH_4, C_2H_4, C_3H_6, CO, and so on.[8] Synthesis of CNTs using polymers as the carbon source is a recently emerging method, and CNTs have been produced, respectively, from polyethylene, poly(vinyl alcohol), blends of poly(methyl methacrylate)/polyacrylonitrile, and polytetrafluoroethene under inert atmosphere.[9] These methods, however, usually require complicated setups and inert gas protection.

Very recently, Tang and co-workers synthesized multiwalled carbon nanotubes (MWNTs) in large quantities by burning a polypropylene/nickel/montmorillonite composite in the atmosphere.[10] This system was applied later to flame retardancy of polypropylene and showed an excellent flame-retardant ability.[11] In this method, however, pre-synthesized nickel nanocatalysts (nickel nanoparticles supported on silica−alumina) are an indispensable component in the composite, otherwise no CNTs are formed.

In this paper, we report a novel in situ approach to the mass production of MWNTs using nickel formate as a catalyst precursor. Chestnut-like spheres of tangled MWNTs were fabricated in high yield without adding any pre-synthesized nickel nanocatalyst. The products were studied by a variety of methods. Finally, the formation mechanism and potentials of the current approach are discussed.

Experimental Procedures

Materials. Nickel formate ($(HCOO)_2Ni{\cdot}2H_2O$, NF) and organomontmorillonite (OMMT, I.44P) were purchased from Alfa Aesar and Nanocor, respectively. Commercially available pellet polypropylene (PP, melt flow index: 2.5 g/10 min) was obtained from Yanshan Chemical Co. $H_2PtCl_6{\cdot}6H_2O$ was purchased from Shenyang Jin-Ke Reagents. Ethylene glycol, nitric acid, and hydrofluoric acid were obtained from Beihua Fine Chemicals. These reagents were used as received.

Fabrication Procedure. In a typical procedure, nickel formate was dehydrated at 160 °C before use. It was then mixed with PP and OMMT in a Brabender mixer at 80 rpm and 180 °C for 7 min. When the temperature of the muffle furnace reached 900 °C, a piece of the mixed composite was placed in a crucible, put in the muffle furnace, and heated at 900 °C for 5 min. The crucible was then allowed to cool to room temperature, and a black powder was obtained. The black powder was immersed into 20% (v/v) hydrofluoric acid for 24 h to remove the montmorillonite. It was then refluxed at 130 °C in aqueous nitric acid (3 M) for 24 h to remove amorphous

* To whom correspondence should be addressed. Tel.: +86-10-82543535; fax: +86-10-82543535; e-mail: jhhe@mail.ipc.ac.cn.
[†] Chinese Academy of Sciences.
[‡] Institute of Chemical Defense.

10.1021/jp064682+ CCC: $33.50
Published on Web 09/26/2006

TABLE 1: Effects of Concentrations of NF and OMMT on Yields of CNTs[a]

sample	PP (wt %)	OMMT (wt %)	catalyst (wt %)	CNT/PP (%)
1	90	10	0	0
2	87.5	10	2.5	1.3
3	85	10	5	50
4	82.5	10	7.5	50
5	95	2.5	2.5	0.8
6	92.5	5	2.5	5.1
7	90	5	5	36

[a] CNT/PP is the mass of obtained CNTs divided by the mass of PP.

carbon and nickel. Varied compositions were studied. The compositions and corresponding MWNT yields are listed in Table 1. Pt nanoparticles were deposited on CNTs as follows. CNTs (5 mg) were mixed with a solution of sodium dodecyl sulfate (2%) in ethylene glycol (18 mL). After sonicating the mixture for 1 h, 2 mL of H_2PtCl_6 in ethylene glycol (2.5 mmol/mL) was added under constant agitation. The reaction mixture was then heated at 140 °C in an oil bath for 30 min under vigorous agitation to ensure completion of the reaction. After two cycles of centrifugation and washing with ethanol, the resulting product was dispersed in ethanol. Transmission electron microscopy (TEM) measurements were carried out on a JEOL JEM-2010 transmission electron microscope operating at an accelerating voltage of 200 kV. X-ray diffractometry (XRD) analysis of the product was carried out on a PGENERAL XD-2 X-ray diffractometer using Cu Kα radiation ($\lambda = 1.5406$ Å). The prepared samples were also observed by scanning electron microscopy (SEM) on a Hitachi S-4300 operating at 10 kV. Raman spectroscopy was acquired using a JY-HR800 Raman spectrometer with an excitation beam wavelength at 532 nm. The N_2 adsorption and desorption at −196 °C were carried out using a Quantachrome Instrument. The sample was degassed at 300 °C in high vacuum before the measurements. The pore size distribution was determined from nitrogen desorption data by the BJH method, and the pore surface area distribution against the pore size was also obtained from nitrogen desorption data by the BJH method.

Results and Discussion

Fabrication of Chestnut-Like Carbon Nanotube Spheres. PP/OMMT/NF composites were prepared by mixing these components in a Brabender mixer. After heating the composites at 900 °C, CNT/montmorillonite (MMT)/Ni composites were obtained. They were further purified with HF and HNO_3. XRD was used to study the crystalline phases of the sample at different stages. Figure 1 shows XRD patterns of the PP/OMMT/NF composite. After heating at 900 °C, the diffraction peaks of PP and OMMT in the composite disappeared. At the same time, two new strong diffraction peaks appeared at 25.8 and 44.5°, which were ascribed to graphitic carbon and metallic nickel, respectively. Thus, NF decomposed to metallic nickel, and PP was converted to graphitic carbon (i.e., CNTs by heating at 900 °C). The in situ formed metallic nickel must have served as the catalyst and nucleus for growth of the CNTs. After purification with HF and HNO_3, the diffraction peak at 44.5° weakened dramatically, indicating that most of the metallic nickel was removed.

In situ formation of nickel nanoparticles by decomposition of NF at 900 °C was confirmed by TEM observations of the unpurified product. Figure 2a shows a TEM image that was obtained by focusing on the Ni nanoparticles. The unclear background is CNT spheres. To observe Ni nanoparticles and

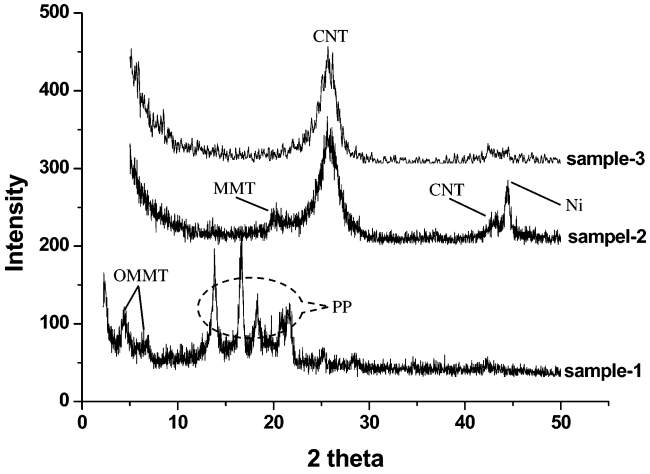

Figure 1. XRD patterns of as-mixed PP/OMMT/NF composite before (sample 1) and after (sample 2) heating at 900 °C and after purification by HF and HNO_3 (sample 3). PP: 85 wt %, OMMT: 10 wt %, and NF: 5 wt %.

CNTs simultaneously, CNT spheres were crushed by ultrasonication and observed again by TEM. As shown in Figure 2b, both Ni nanoparticles and CNTs were observed. Each Ni nanoparticle is located at the end of CNT. Clearly, the in situ formed Ni nanoparticles acted as nanocatalysts for the growth of CNTs. It was known that nickel formate dehydrates at 160 °C and decomposes at 260 °C. The decomposition proceeds by a self-redox reaction, resulting in metallic nickel and gas species (H_2 and CO_2).[7b,12] It was reported that nickel particles could be obtained at a residence time as short as 0.1 s at 600 °C.[12b] The mean diameter (d) and standard deviation (σ) of Ni nanoparticles were estimated, and they are ca. 19.9 and ca. 8.5 nm, respectively. These in situ synthesized nickel nanoparticles fall in the size range that is suitable for the growth of CNTs and are believed to be more catalytically active than pre-synthesized Ni catalysts.

Figure 3 shows SEM images of the obtained product before and after purification with hydrofluoric acid and nitric acid. Chestnut-like spheres were observed before purification (Figure 3a). This morphology was in contrast to that obtained by using pre-synthesized nickel nanocatalysts;[10] the latter was basically irregular. Their diameters are in the range of 6−7 μm. Surrounding these spheres are exfoliated montmorillonite platelets, either on the spheres or beside them. Figure 3b is a magnified SEM image of a sphere with some montmorillonite platelets. Clearly, the sphere is composed of CNTs that impart a chestnut-like morphology. Figure 3c shows a SEM image of the product after purification. Clearly, montmorillonite platelets were completely removed. A magnified image (Figure 3d), however, indicates that the CNTs were kept intact. The diameter of the CNTs was estimated to be ca. 30 nm.

Figure 4a shows a low-magnification TEM image of the CNTs from PP/OMMT/NF. Hollow tubular structures are clearly seen. The CNTs extend to micrometers in length and are tangled with each other. The outer and inner diameters are 25−50 and 5−10 nm, respectively. The tube wall has a thickness of 10−20 nm and is thicker than the inner diameter. Figure 4b shows a magnified image of two nanotubes (37.6−40 nm in diameter) that cross with each other. Clearly, the two individual nanotubes are not fused with each other at the cross-section. Figure 4c is a high-resolution TEM (HRTEM) image of a single CNT. The CNT wall is composed of stacked graphite sheets aligned nearly along the axis of the tube. It was noted that the innermost and outermost walls do not have a regular graphitic structure. Such

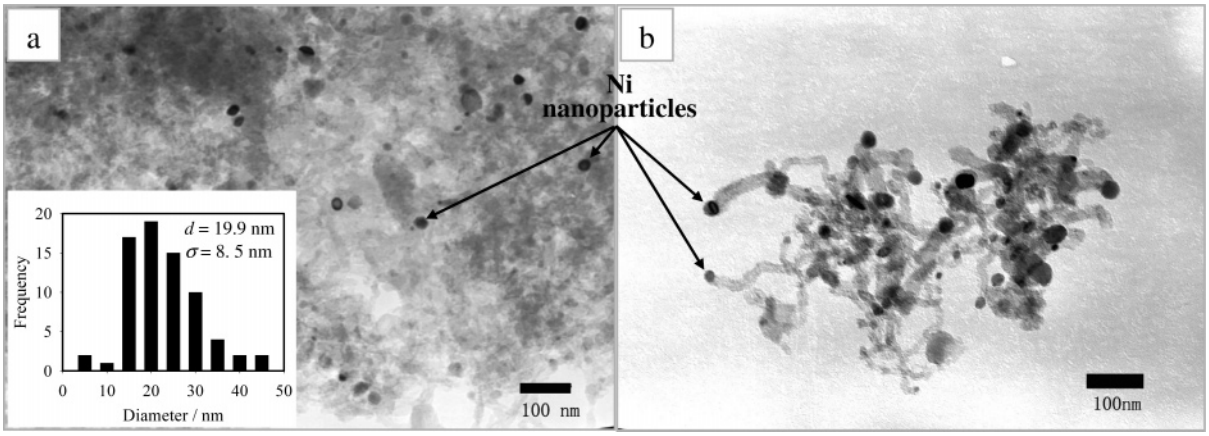

Figure 2. TEM images (a and b) of Ni nanopariticles in situ formed by decomposition of PP/OMMT/NF at 900 °C. The inset in panel a is the histogram of Ni nanoparticles. PP: 85 wt %, OMMT: 10 wt %, and NF: 5 wt %.

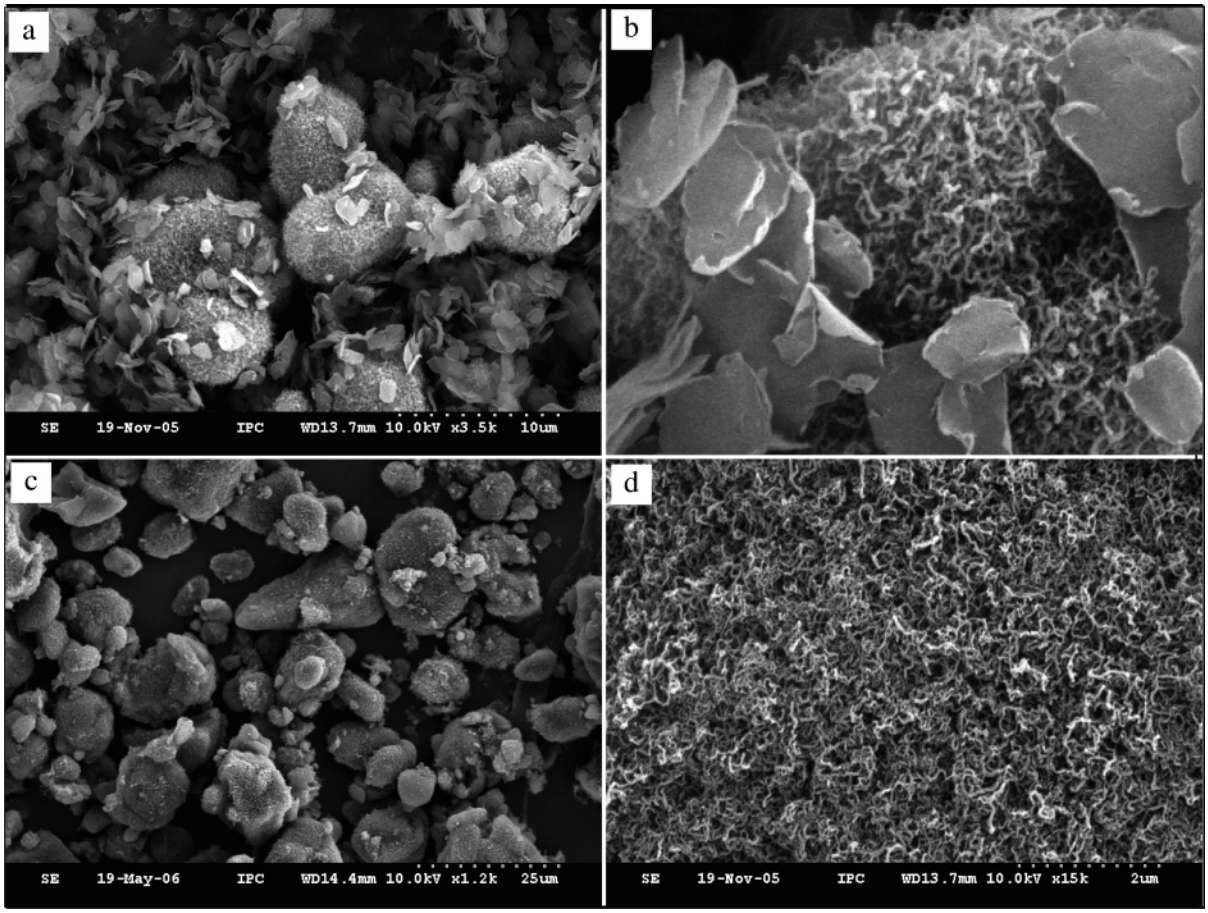

Figure 3. SEM images of as-prepared chestnut-like carbon nanotube spheres before (a and b) and after (c and d) purification by HF and HNO_3. PP: 85 wt %, OMMT: 10 wt %, and NF: 5 wt %.

structural irregularity was probably induced during the purification process with nitric acid.

The purified CNTs were also studied by Raman spectroscopy. As shown in Figure 5, two strong peaks appear at 1590 and 1346 cm^{-1}, respectively, in the Raman spectrum. The former (so-called G-band) is attributed to an E_{2g} mode of hexagonal graphite and is associated with the vibration of sp^2-hybridized carbon atoms in a graphite layer. The latter (so-called D-band) is ascribed to the vibration of carbon atoms with dangling bonds in the plane terminations of disordered graphite.[13] Such disordered structures might originate from the purification process. Thus, the Raman spectroscopic results agree with the HRTEM observations. Two weak peaks also appear in a higher frequency range, which are attributed, respectively, to the double frequencies of the D- and G-bands.

The surface area and mesoporosity of the CNT spheres after acid treatment were revealed by N_2 adsorption−desorption measurements. Obtained isotherms are shown in Figure 6a. They are of typical type IV with a hysteresis loop, representative of mesoporosity based on the IUPAC nomenclature. Considering the geometry of MWNTs, MWNT samples are assumed to contain cylindrical pores and no pore networks, thus satisfying the two main requirements of the BJH method. The pore size distribution was derived from the adsorption branch of the isotherms. As shown in Figure 6b, it has two peaks, one located below 1 nm and the other between 1 and 10 nm. The former

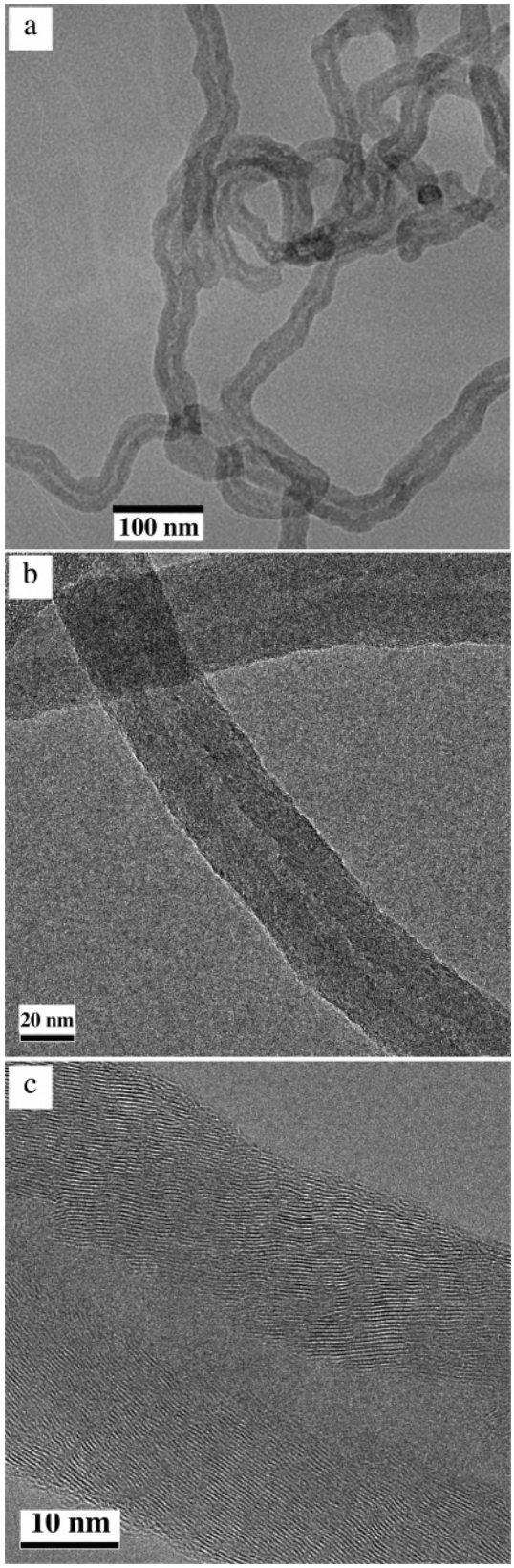

Figure 4. TEM images of purified MWNTs (a and b) and HRTEM image of individual MWNT. PP: 85 wt %, OMMT: 10 wt %, and NF: 5 wt %.

was assigned to the cylindrical pores of CNTs of small inner diameter, the latter to both the cylindrical pores of CNTs of a larger inner diameter and the intertube space. The previously results suggest that the CNT spheres contain abundant mesopores. From Figure 6, the total surface area and pore volume

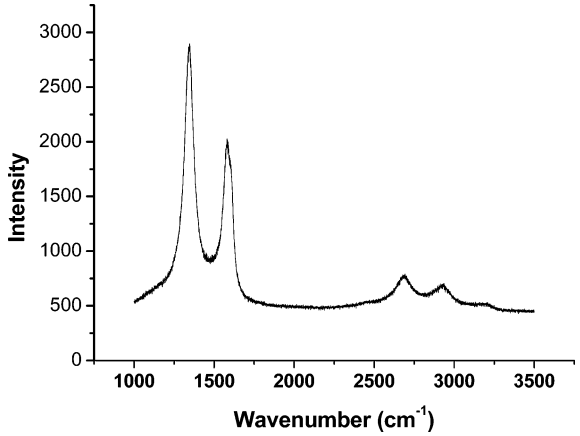

Figure 5. Raman spectrum of purified MWNTs obtained from PP/OMMT/NF. PP: 85 wt %, OMMT: 10 wt %, and NF: 5 wt %.

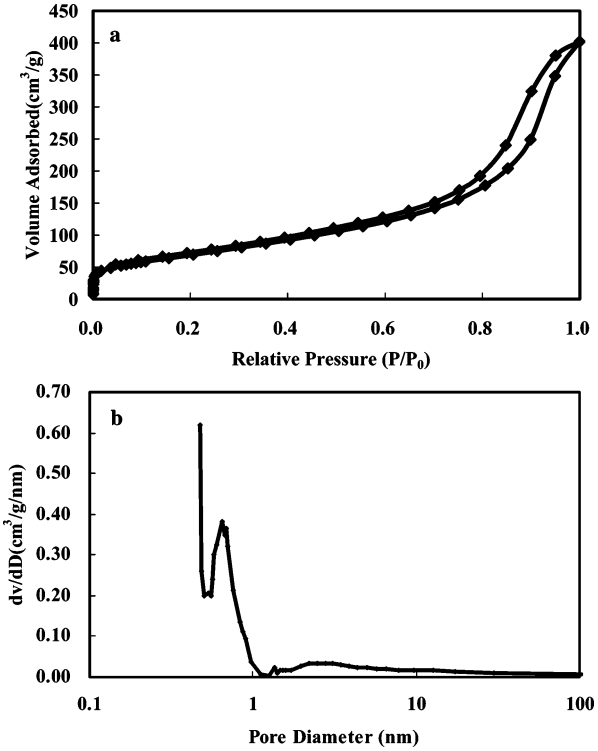

Figure 6. N_2 adsorption−desorption isotherms (a) and the corresponding pore size distribution curve as calculated by the BJH method. PP: 85 wt %, OMMT: 10 wt %, and NF: 5 wt %.

were calculated to be 250 m^2/g and 0.5877 cm^3/g, respectively. It was observed that in the acid treatment, several functional groups such as the hydroxy, carboxy, and carbonyl groups are formed on the surface of the nanotubes. This high surface area is at least partially attributed to the acid treatment.[14] The high surface area indicates the possibility of these CNTs as catalyst supports.

Effects of Concentrations of NF and OMMT, Heating Temperature, and Time on Yields of CNTs. The effects of the catalyst precursor (NF) and the additive (OMMT) were also investigated by varying their concentrations. The results are summarized in Table 1. The yield of CNTs is defined as the mass of obtained CNTs divided by the mass of PP (CNT/PP). When the concentration of OMMT was kept at 10 wt %, an increase of the NF concentration from 0 to 5 wt % led to an increase of the CNT yield from 0 to 50% (samples 1−3). Further increase of the NF concentration to 7.5 wt %, however, did not cause a noticeable change of the CNT yield (sample 4). On the

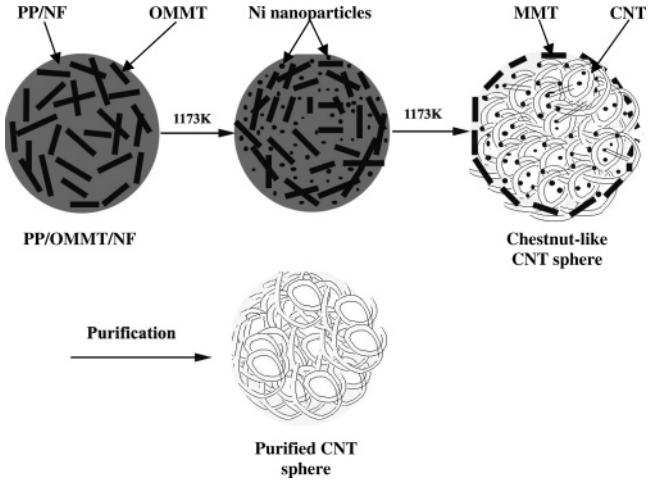

Figure 7. Proposed formation mechanism of chestnut-like CNT spheres.

other hand, when the concentration of NF was kept at 2.5 wt %, an increase of OMMT from 2.5 to 5 wt % gave rise to an increase of the CNT yield from 0.8 to 5.1% (samples 5 and 6). However, the CNT yield dropped to 1.3% when the concentration of OMMT further increased to 10 wt % (sample 2). In contrast, at a higher NF concentration of 5 wt %, an increase of the OMMT concentration from 5 to 10 wt % led to an increase of the CNT yield from 36 to 50%. These results indicate that both OMMT and NF were involved in the synthesis of CNTs. The 10 and 5 wt % were thus used as optimum OMMT and NF concentrations, respectively, for other experiments.

Heating temperature and heating time also affected the formation of chestnut-like MWNTs. At 500, 700, and 900 °C, the CNT yields were 6.2, 41.8, and 50%, respectively (i.e., the CNT yield increased with increasing the heating temperature). However, morphological changes were not significant except for the length of the CNTs. Longer CNTs were obtained at higher temperatures. On the other hand, the required times for completion of the reaction at 500, 700, and 900 °C were 8, 5, and 5 min, respectively. It must be pointed out that when the heating time at 900 °C was further lengthened, the produced CNTs were oxidized eventually, leaving only MMT.

Formation Mechanism of CNTs. It is important to discuss the formation mechanism of MWNTs from the current PP/OMMT/NF composite. On the basis of the previous discussion, a formation mechanism was proposed, as shown in Figure 7. PP and OMMT are known to form spherulites of PP/OMMT under heating conditions.[15] In the process of Brabender mixing, PP and OMMT may form spherulites that contain NF. When the PP/OMMT/NF composite is placed in an oven at 900 °C, nickel formate decomposes instantly, giving a large number of nickel nanoparticles within the spherulites. Meanwhile, OMMT platelets migrate to the surface of spherulites due to temperature and viscosity gradients, gas formation, interfacial tension between OMMT and PP, and surface free energy of the polymer.[16] PP pyrolyzes to give pyrolytic species that are sealed in an autoclave-like microreactor formed by OMMT plallets.[10] Within the autoclave-like microreactor, the pyrolytic species are catalyzed to form CNTs on these nickel nanoparticles. The confinement of the microreactor results in curled CNTs and eventually in chestnut-like spheres. It is very interesting that at identical concentrations of PP (85 wt %), OMMT (10 wt %), and catalyst (5 wt %), the current method gave 50 wt % MWNTs (sample 3 in Table 1), nearly 9 wt % higher than the previously reported method.[10]

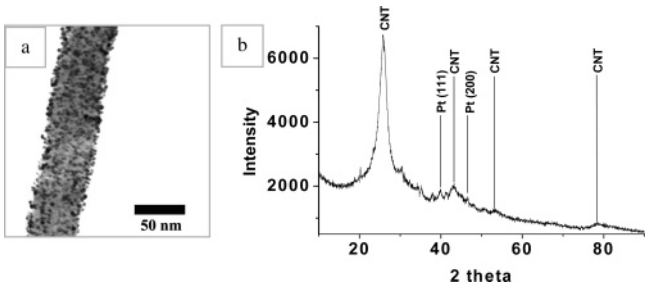

Figure 8. TEM image (a) and XRD pattern (b) of CNT-supported Pt nanoparticles. PP: 85 wt %, OMMT: 10 wt %, and NF: 5 wt %.

Chestnut-Like CNT Spheres as a Support of Pt Nanoparticles. Direct synthesis of nanoparticles on solid matrixes is attracting increasing interest in terms of practical applications and synthetic challenges.[17−25] The chestnut-like CNT spheres prepared by the current approach are on the micrometer size scale and are thus easily separated by conventional filtration. On the other hand, the spheres have a large surface area (ca. 250 m^2/g). These characteristics make them promising as a catalyst support. Therefore, we explored the possibility of depositing Pt nanoparticles on CNTs. As shown in Figure 8a, Pt nanoparticles were successfully deposited on the outer surface of CNT. The mean diameter and its standard deviation of Pt nanoparticles were estimated to be ca. 2.64 and ca. 0.62 nm, respectively. The crystalline nature of the Pt nanoparticles was confirmed by XRD measurements. Figure 8b shows the XRD pattern of the Pt/CNT composite. The peak at 26.5° corresponds to graphitized CNTs, and the peaks at 39.7 and 46.2° could be assigned to the (111) and (200) planes of metallic Pt, indicating that the Pt nanoparticles are composed of pure crystalline Pt. It was reported that freshly formed Pt monomers and CNT surfaces could form strong bonds that promote heterogeneous nucleation followed by formation of Pt nanoparticles on CNTs.[26] The surface functional groups might also contribute to the stabilization of Pt nanoparticles on CNTs. According to the literature,[14b] Pt nanoparticles were located on CNTs, which would lead to the decrease of the mesopore condensation. Comparing our experimental conditions to those in the literature, we could estimate that nearly 20% of those pores between 1 and 10 nm were occupied by Pt nanoparticles.

Conclusion

In summary, we reported a novel in situ approach to mass fabrication of chestnut-like carbon nanotube spheres from polypropylene and nickel formate. The indication of these results is at least 2-fold. First, instead of using a pre-synthesized nanocatalyst, the current method uses a catalyst precursor in combination with PP and OMMT. Ni nanoparticles are in situ formed within the composite and catalyze the formation of MWNTs in an autoclave-like microreactor formed by OMMT. Such in situ formed Ni nanoparticles are shown to be more catalytically active than pre-synthesized nickel nanocatalysts, resulting in higher CNT yields. Thus, the synthetic procedure of metal nanocatalysts can be eliminated. Second, the current method is facile and allows easy and low-cost synthesis of carbon nanotubes on a large scale. The matrix polymer may not be limited to polypropylene. It may also be recycled polyolefins and their composites. Thus, the current approach may be used to convert polyolefin wastes (so-called white rubbish) to advanced carbon materials. On the other hand, the current finding may also be promising for polyolefin flame retardancy. The obtained CNT spheres have a high surface area, which makes them a good catalyst support. Successful deposi-

tion of Pt nanoparticles in the CNT spheres provides opportunities to study these possibilities. The applications of CNT sphere-supported Pt nanoparticles in chemical reactions are currently being studied in our laboratory.

Acknowledgment. This work was supported by the National Natural Science Foundation of China (Grant 20471065), "Hundred Talents Program" of CAS, and the President Fund of CAS. We are grateful to M. Zhong and Q. Cheng of PGENERAL for the XRD measurements.

References and Notes

(1) Dresselhaus, M. S., Dresselhaus, G., Avouris, P., Eds.; *Carbon Nanotubes*: *Synthesis, Structure, Properties, and Applications*; Springer: New York, 2002.

(2) Ebbesen, T. W.; Ajayan, P. M. *Nature* **1992**, *358*, 220.

(3) Thess, A.; Lee, R.; Nikolaev, P.; Dai, H.; Petit, P.; Robert, J.; Xu, C. H.; Lee, Y. H.; Kim, S. G.; Rinzler, A. G.; Colbert, D. T.; Scuseria, G. E.; Tomanek, D.; Fischer, J. E.; Smalley, R. E. *Science* **1996**, *273*, 483.

(4) Ren, Z. F.; Huang, Z. P.; Xu, J. W.; Wang, J. H.; Bush, P.; Siegal, M. P.; Provencio, P. N. *Science* **1998**, *282*, 1105.

(5) (a) Shi, Z.; Lian, Y.; Zhou, X.; Gu, Z.; Zhang, Y.; Iijima, S.; Li, H.; Yue, K. T.; Zhang, S.-L. *J. Phys. Chem. B* **1999**, *103*, 8698. (b) Yudasaka, M.; Komatsu, T.; Ichihashi, T.; Achiba, Y.; Iijima, S. *J. Phys. Chem. B* **1998**, *102*, 4892.

(6) (a) Qin, L. C. *J. Mater. Sci. Lett.* **1997**, *16*, 457. (b) Fan, Y.-Y.; Li, F.; Cheng, H.-M.; Su, G.; Yu, Y.-D.; Shen, Z.-H. *J. Mater. Res.* **1998**, *13*, 2342.

(7) (a) Geng, J.; Li, H.; Golovko, V. B.; Shephard, D. S.; Jefferson, D. A.; Johnson, B. F. G.; Hofmann, S.; Kleinsorge, B.; Robertson, J.; Ducati, C. *J. Phys. Chem. B* **2004**, *108*, 18446. (b) Geng, J. F.; Singh, C.; Shephard, D. S.; Shaffer, M. S. P.; Johnson, B. F. G.; Windle, A. H. *Chem. Commun.* **2002**, 2666.

(8) (a) Nolan, P. E.; Lynch, D. C.; Cutler, A. H. *J. Phys. Chem. B* **1998**, *102*, 4165. (b) Che, G.; Lakshmi, B. B.; Martin, C. R.; Fisher, E. R.; Ruoff, R. S. *Chem. Mater.* **1998**, *10*, 260. (c) Kyotani, T.; Tsai, L.-F.; Tomita, A. *Chem. Mater.* **1996**, *8*, 2109. (d) Zheng, B.; Lu, C.; Gu, G.; Makarovski, A.; Finkelstein, G.; Liu, J. *Nano Lett.* **2002**, *2*, 895.

(9) (a) Kukovitskii, E. F.; Chernozatonskii, L. A.; L'vov, S. G.; Mel'nik, N. N. *Chem. Phys. Lett.* **1997**, *266*, 323. (b) Maksimova, N. I.; Krivoruchko, O. P.; Mestl, G.; Zaikovskii, V. I.; Chuvilin, A. L.; Salanov, A. N.; Burgina, E. B. *J. Mol. Catal.* **2000**, *158*, 301. (c) Krivoruchko, O. P.; Maksimova, N. I.; Zaikovskii, V. I.; Salanov, A. N. *Carbon* **2000**, *38*, 1075. (d) Hulicova, D.; Hosoi, K.; Kuroda, S.-I.; Abe, H.; Oya, A. *Adv. Mater.* **2002**, *14*, 452. (e) Huczko, A.; Lange, H.; Chojecki, G.; Cudzilo, S.; Zhu, Y. Q.; Kroto, H. W.; Walton, D. R. M. *J. Phys. Chem. B* **2003**, *107*, 2519.

(10) Tang, T.; Chen, X. C.; Meng, X. Y.; Chen, H.; Ding, Y. P. *Angew. Chem., Int. Ed.* **2005**, *44*, 1517.

(11) Tang, T.; Chen, X. C.; Chen, H.; Meng, X. Y.; Jiang, Z. W.; Bi, W. G. *Chem. Mater.* **2005**, *17*, 2799.

(12) (a) The Merck Index, 13th ed.; Merck Research Laboratories, Division of Merck and Co., Inc.: Whitehouse Station, NJ, 2001; p 1166. (b) Xia, B.; Lenggoro, I. W.; Okuyama, K. *J. Am. Ceram. Soc.* **2001**, *84*, 1425.

(13) Rao, A. M.; Richter, E.; Bandow, S.; Chase, B.; Eklund, P. C.; Willams, K. A.; Fang, S.; Subbaswamy, K. R.; Menon, M.; Thess, A.; Smalley, R. E.; Dresselhaus, G.; Dresselhaus, M. S. *Science* **1997**, *275*, 187.

(14) (a) Kanyo, T.; Konya, Z.; Kukovecz, A.; Berger, F.; Dekany, I.; Kiricsi, I, *Langmuir* **2004**, *20*, 1656; (b) Ovejero, G.; Sotelo, J. L.; Romero, M. D.; Rodríguez, A.; Ocaña, M. A.; Rodríguez, G.; García, J. *Ind. Eng. Chem. Res.* **2006**, *45*, 2206.

(15) Ma, J. S.; Zhang, S. M.; Qi, Z. N.; Li, G.; Hu, Y. L. *J. Appl. Polym. Sci.* **2002**, *83*, 1978.

(16) Lewin, M.; Pearce, E. M.; Levon, K.; Mey-Marom, A.; Zammarano, M.; Wilkie, C. A.; Jang, B. N. *Polym. Adv. Technol.* **2006**, *17*, 226.

(17) He, J.; Kunitake, T. In *Nanocrystals Forming Mesoscopic Structures*; Pileni, M.-P., Ed.; Wiley-VCH: Weinheim, 2005; pp 91−118.

(18) He, J.; Ichinose, I.; Kunitake, T.; Nakao, A. *Langmuir* **2002**, *18*, 10005.

(19) He, J.; Ichinose, I.; Fujikawa, S.; Kunitake, T.; Nakao, A. *Chem. Commun.* **2002**, *17*, 1910.

(20) He, J.; Kunitake, T.; Nakao, A. *Chem. Mater.* **2003**, *15*, 4401.

(21) He, J.; Ichinose, I.; Kunitake, T.; Nakao, A.; Shiraishi, Y.; Toshima, N. *J. Am. Chem. Soc.* **2003**, *125*, 11034.

(22) He, J.; Kunitake, T.; Nakao, A. *Chem. Commun.* **2004**, 410.

(23) He, J.; Kunitake, T. *Chem. Mater.* **2004**, *16*, 2656.

(24) (a) Liu, S.; He, J. *J. Am. Ceram. Soc.* **2005**, *88*, 3513. (b) Giermann, A. L. *MRS Bull.* **2006**, *31*, 79.

(25) Li, C.; He, J. *Langmuir* **2006**, *22*, 2827.

(26) Wang, Y.; Xu, X.; Tian, Z.; Zong, Y.; Cheng, H.; Lin C. *Chem. Eur. J.* **2006**, *12*, 2542.